Proceedings of the Combustion Institute, Volume 28, 2000/pp. 1639–1646

ZERO-DIMENSIONAL ANALYSIS OF DILUTED OXIDATION OF METHANE IN RICH CONDITIONS

MARIAROSARIA DE JOANNON,[1] ALESSANDRO SAPONARO[2] AND ANTONIO CAVALIERE[1]
[1]*Dipartimento di Ingegneria Chimica*
Università Federico II
Napoli, Italy
[2]*Centro Combustione-Ansaldo-Termosud*
Gioia del Colle
Bari, Italy

Clean combustion technologies, based on reactant dilution, have shown very peculiar and innovative characteristics. Reduction of light and noise emission and uniformity of temperature and composition distribution inside the combustion chamber, related to an extension of the reaction zone, make these processes very promising in several technological fields. Analysis of combustion in very diluted conditions is needed for a general understanding of these processes, which remain unknown from many aspects. The study is also useful for the identification of practical constraints which define the most suitable reactor configurations and working parameters for process reliability.

The present work deals with a theoretical analysis of methane oxidation in diluted conditions using one of the detailed kinetic schemes available in the literature. A well-stirred reactor (WSR) configuration has been considered as a first attempt of process schematization. This choice is consistent with the experimental characterization of the flameless combustion processes.

The influence of residence time, C/O ratio, and inlet temperature on the steady state was studied for an oxygen molar fraction (0.05), chosen as representative of flameless combustion processes. It has been pointed out that only rich conditions (C/O $>$ 0.25) are possible for WSR creation, because they allow partial methane conversion. Three kinetic regimes, related to different temperature ranges, have been identified on the basis of product distribution analysis.

Both the oxidation and pyrolitic regimes, occurring respectively in low- and high-temperature ranges, are the most interesting working conditions for diluted combustion. The former, leading to CO and H_2O as main reaction products, is suitable for reburning technology. The latter, which corresponds to large production of CO and H_2, has been shown to be a reasonable explanation of flameless combustion.

Advantages and potentials of this innovative process are analyzed, taking into account the kinetic pathway followed in the different working conditions.

Introduction

The dilemma concerning the well-stirred reactor (WSR) feasibility is posed at present by recent development of innovative combustors [1–6] fed by high temperature air [1,2] that yield a noiseless, colorless, or narrow band emission [2,4] process which is also named flameless combustion [6]. Quite uniform temperature and composition fields have also been documented when the temperature is increased beyond a threshold level in a furnace, fed by methane and air [2,5,6]. This suggests that the diffusion-controlled combustion changes into a kinetic-controlled process and some preliminary calculations seem to show that the outlet WSR conditions are reached [3]. This has also been partially confirmed by a numerical analysis with simplified two-step kinetics [7] which shows a tendency to partial conversion of the methane/oxygen systems, when diluted conditions are taken into account.

Since most of the acquired knowledge for the combustion of methane has been included in the models and tested in several conditions, the comprehensive assessment of relatively distant regimes is today possible on the ground of quantitative, repeatable computations for such systems. In fact, detailed kinetics schemes [8–10] have been developed and tested in the past two decades through cooperative efforts in different applications (e.g., ignition, premixed flames, diffusion flames) for methane/air combustion.

This paper deals with an application of one of these schemes in a WSR in order to understand whether there are theoretical limits which cannot be exceeded, even though the well-known practical constraints are overcome. Different boundary conditions in terms of temperature and composition are considered in this paper in order to evaluate the real conditions of the flameless occurrence. An example

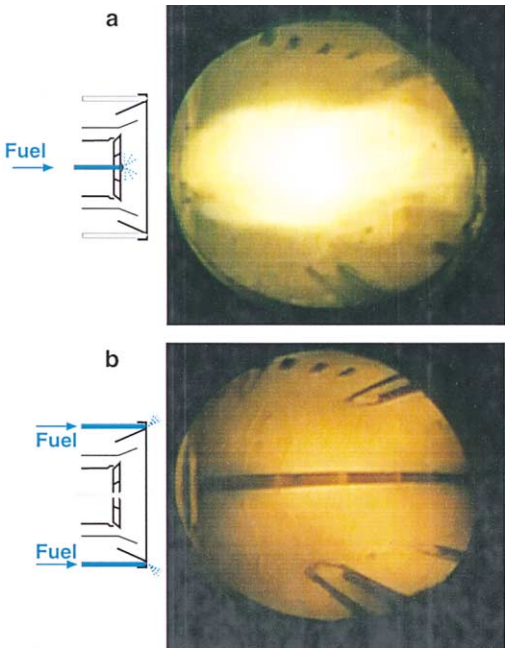

FIG. 1. (a) Traditional natural gas flame. (b) Natural gas flameless combustion.

of this type of process is outlined in the following section with the purpose of stressing some features of technological interest.

Example of Flameless Combustion

A facility of 48 MWth of thermal power has been used to run tests of natural gas combustion with different fluid-dynamic configurations. The fuel volume flowrate was kept constant at 3000 Nm^3/h. The airflow at $T = 600$ K was fed in such a way that the oxygen in the flue gas was 0.8%, with CO less than 100 ppm. The main burner configuration is outlined schematically on the left side of Fig. 1a. It consists of confinement of three coaxial fluxes with tailored swirl levels. The fuel is injected through 43 outlet holes, placed on one central spud and grouped in cylindrical rows tilted in the symmetrical plane at 30°, 60°, and 90° with respect to the cylindrical axis. The blue lines in the figure represent these orientations.

Such configuration yields a diffusion-controlled flame with shape and visible emission of traditional characteristics. The yellow compact region, shown in Fig. 1a, is placed around the axis and extends for the whole chamber.

The second configuration is outlined on the left side of Fig. 1b. The natural gas, depicted with blue color, is injected through eight spuds placed on the cylindrical surface. The distance of the spud head from the symmetry axis and from the burner outlet has been settled by means of cold fluid-dynamic studies on the external side of the most external air jets on the border of the outward reverse flow. Four nozzle holes on each spud were oriented in such a way that they take into account the enlargement and the rotation of the external swirl. Details are not relevant, but the main characteristic of the fuel injection into a flue gas recirculation zone should be emphasized in order to appreciate the statements presented in the discussion.

The most striking characteristic of the new combustion regime is revealed by the visual observation of the combustion chamber. Fig. 1b shows details of the internal part of the combustion chamber. In fact, it is possible to observe the hopper, which is on the bottom of the chamber and the walls, which are slightly emitting due to the refractory coating. Visible emission is practically negligible and, according to the narrowest dynamic range of the detection–digitization device, it can be detected smaller than any part of the previous flames of two order of magnitudes. This means that not only soot but also the bluish emission due to CH and $CO_2^T \rightarrow CO_2^S$ chemiluminescence are completely absent.

Fuel injection in intermediate positions did not result in this dramatic change, whereas air vitiation with exhaust gas recirculation did not affect the second colorless combustion.

WSR Configuration

A theoretical analysis of methane oxidation evolving in an adiabatic WSR configuration has been done considering several boundary conditions. An oxygen molar fraction (X_{O_2}) of 0.05 has been chosen as representative of flameless combustion conditions. The influence of residence time (τ), C/O ratios, inlet temperature (T_o) on outlet temperature (T_{wsr}), and product distribution has been investigated. Methane oxidation has been modeled by means of the mechanism proposed by Warnatz (40 species and 170 reactions) [11] and reported in its documented form [9]. Calculations have been performed using the WSR configuration (PSR) [12] of the CHEMKIN package [13].

In Fig. 2, T_{wsr} computed in different conditions has been reported as function of T_o. The green continuous line describes the T_{wsr} profile calculated for C/O = 0.25 and $\tau = 1$ s. It shows a very pronounced S shape associated to the multiplicity of steady-state solutions. In fact, for T_o lower than 950 K, in addition to the isothermal solutions ($T_{wsr} = T_o$, corresponding to a fractional conversion equal to zero for adiabatic conditions), there are two other possible T_{wsr}. They are related to a low and a high conversion level, corresponding to an intermediate and high

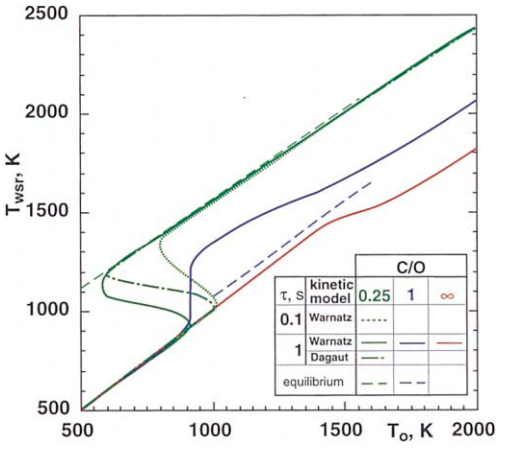

FIG. 2. Working temperature (T_{wsr}) versus inlet temperature (T_o) for methane oxidation in a WSR at X_{O_2} = 0.05 for different τ and C/O ratios.

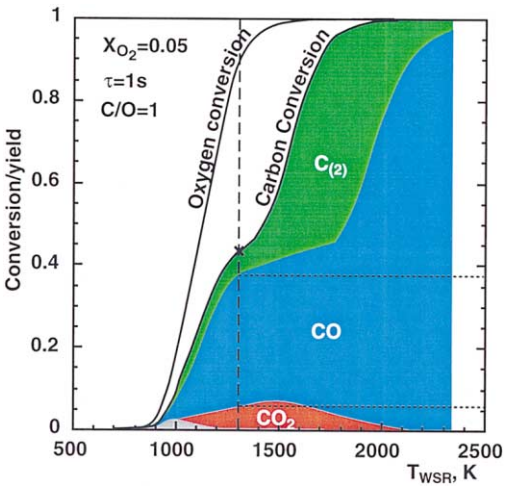

FIG. 3. Solid black lines, oxygen and carbon conversions; gray area, carbon yield to oxygenated compounds; red area, carbon yield to CO_2 (Y_{CO_2}); blue area, carbon yield to CO (Y_{CO}); green area, carbon yield to $C_{(2)}$ ($Y_{C_{(2)}}$); computed at X_{O_2} = 0.05, τ = 1 s, C/O = 1.

working temperature. This zone extends between 600 and 950 K. For temperatures higher than 950 K, there is a single steady-state solution, associated with a unitary fractional conversion. This solution also identifies the equilibrium condition such as shown by the equilibrium data represented in Fig. 2 for C/O = 0.25, by means of the green dashed line.

These data have been compared with results computed by means of other methane oxidation mechanisms, such as the GRI [8] and Dagaut [14] schemes. Solutions calculated with the Dagaut scheme are reported in Fig. 2 with the green dashed-dotted line. High-temperature solutions ($T_o > 1000$ K) coincide with the data obtained with the Warnatz kinetic model, whereas some differences can be found in the low-temperature range. However, solutions of both oxidation models show a nearly similar trend, and they can be considered equivalent with respect to the aim of the present work. Therefore, in the following, the Warnatz mechanism has been used for the theoretical analysis presented here.

The green dotted line of Fig. 2, representing the data at τ = 0.1 s, is similar to the curve for τ = 1 s. In this case, the multiplicity of the steady-state solution occurs between 800 K and 1000 K, slightly shifted with respect to the multiplicity zone identified for longer τ. For $T_o > 1000$ K, the single steady-state solutions again lay on the equilibrium line.

Different behavior can be identified for higher C/O ratios. In Fig. 2, solutions for C/O = 1 and τ = 1 s have been reported (blue continuous line). The curve does not show multiple steady-state solutions, although it retains the S-shape feature. At $T_o < 850$–900 K, the working condition corresponds to the isothermal solution (i.e., zero fractional conversion). The system achieves the steady state for a T_{wsr} just 400 K higher than T_o, in the temperature range between 900 and 1200 K. In this case, the T_{wsr} is higher than the equilibrium temperature (dashed blue line) that, in turn, is very close to the isothermal condition. At higher T_o, the difference between T_{wsr} and T_o decreases until the system reaches equilibrium at about 1600 K.

The temperature profile for C/O = ∞ and τ = 1 s is reported on the same plot with the red line. In this case, $T_{wsr} = T_o$ up to T_o = 1500 K, whereas T_{wsr} is lower than T_o for higher inlet temperatures.

In Fig. 3, the oxygen and carbon conversion calculated for C/O = 1 and τ = 1 s have been reported as function of T_{wsr}. They represent the ratio between the converted and initial moles of atomic oxygen and carbon, respectively. The colored areas under the carbon conversion curve represent the carbon yield of main species (Y_i), which is the fraction of carbon moles converted to the species i. In the figure, the carbon yield to CO_2 (red area), CO (blue area), and $C_{(2)}$ (green area) has been shown. The latter category of species includes all radical and stable compounds, which contain two carbon atoms, that is, products of recombination reactions.

For $T_{wsr} < 1300$ K (evidenced by the dashed line), CO is the main reaction product. In fact, at this temperature, a carbon fractional conversion of about 0.43 (marked with black cross on Fig. 3) corresponds to Y_{CO} of about 0.3 (which represents the segment intercepted on the yield axis by the two dotted lines), whereas both Y_{CO_2} and $Y_{C_{(2)}}$ are about 0.075. In these conditions, the oxygen is completely converted to products, as showed by its conversion curve. The

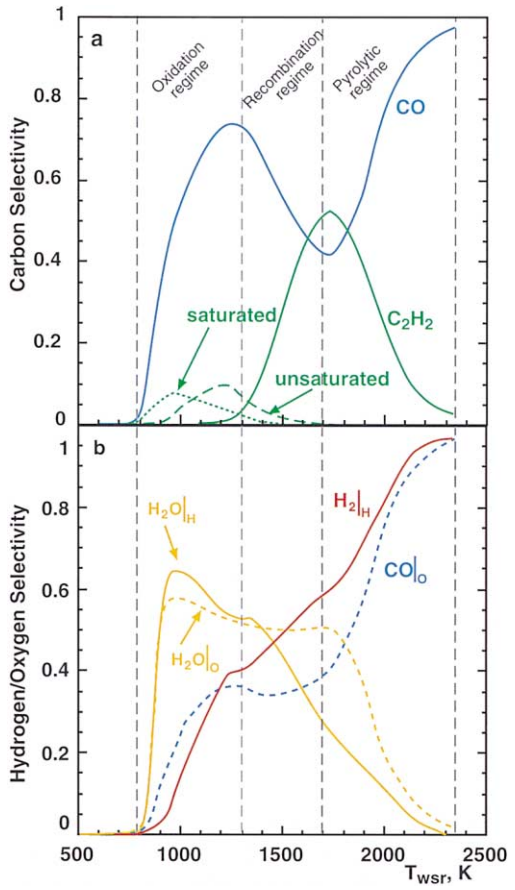

FIG. 4. (a) Carbon selectivity to CO (blue line), C_2H_2 (solid green line), saturated $C_{(2)}$ (dotted green line), unsaturated $C_{(2)}$ (dashed green line). (b) Oxygen selectivity to CO (dashed blue line) and H_2O (dashed yellow line); hydrogen selectivity to H_2 (red line) and H_2O (solid yellow line), as function of T_{wsr} computed at $X_{O_2} = 0.05$, $\tau = 1$ s, C/O = 1.

small gray area present around 1000 K represents the carbon yield for hydrocarbon species containing oxygen atoms (CH_2O, CH_3O, etc.). For temperatures between 1300 and 1750 K, Y_{CO_2} and Y_{CO} are quite constant, whereas $Y_{C_{(2)}}$ increases up to 0.35. A further temperature increase makes $Y_{C_{(2)}}$ and Y_{CO_2} decrease, while both Y_{CO} and carbon conversion increase.

The dependence of product distribution on working temperature can be better analyzed following the selectivity of such species that characterize the main reaction pathway. The selectivity of a species i to a compound j represents the fraction of the reacted moles of i species converted into the compound j. In Fig. 4a, the carbon selectivity to CO and $C_{(2)}$ have been reported as function of T_{wsr}. The C selectivity to CO (blue curve) reaches 0.75 in the temperature range between 800 and 1300 K, in agreement with the yields of Fig. 3. It drops to 0.4 until 1700 K, and then it rises up to the equilibrium condition.

The C selectivity to $C_{(2)}$ has been represented by means of its three components, which are the contributions of acetylene (solid green line), saturated compounds (dotted green line), and unsaturated compounds (dashed green line). Saturated and unsaturated $C_{(2)}$ are present, as secondary reaction products, between 800 and 1400 K. Their selectivities attain the maximum value of 0.1, at about 1000 K and 1200 K, respectively. A large contribution to the C selectivity to $C_{(2)}$ is due to C_2H_2. Starting from 1300 K, it increases with T_{wsr} up to its maximum of 0.55 for $T_{wsr} = 1700$ K. This maximum occurs in correspondence with the minimum of carbon selectivity to CO. At higher temperature, C_2H_2 decreases until it achieves its equilibrium value nearly equal to zero.

The CO formation can also be analyzed in terms of oxygen selectivity, reported with the dashed blue line in Fig. 4b. It increases with working temperature up to $T_{wsr} = 1300$ K, then it flattens at 0.35 until $T_{wsr} = 1700$ K. In this temperature range, between 1300 and 1700 K, the O selectivity to H_2O (yellow dashed line of Fig. 4b) also shows a flat zone that corresponds to a value of about 0.55. Then it goes down to zero, whereas the O selectivity to CO increases again up to the equilibrium value.

A monotone trend characterizes the H selectivity to H_2 (red line) that increases with T_{wsr} over the whole temperature range. Moreover, the H selectivity to H_2O (yellow solid line) rises up to 0.65 for $T_{wsr} = 1000$ K, then it decreases down to zero, apart from a shoulder at 1300 K.

The influence of the diluent composition is shown in Fig. 5 where the yields computed considering $N_2/CO_2/H_2O$ mixture (0.65/0.067/0.133) are reported. These yields have been evaluated with respect to the total carbon atoms fed (as both CH_4 and CO_2). In this case, they are also represented with colored areas by using the same color code as Fig. 3, and their values can be read on the left-hand axis. Y_{CO_2} reaches 0.43 between 900 and 1400 K, and then it decreases to 0.2. Y_{CO} is represented by the ensemble of the plain, dashed, and dotted blue areas. By associating this domain to the left-hand axis, it can be shown that Y_{CO} increases over the whole temperature range. If the dotted blue region is related to the right-hand axis, as it is indicated by the arrow, it represents Y_{CO} obtained using pure nitrogen as diluent, already reported in Fig. 3. The plain and dashed regions represent the contribution to Y_{CO} due to the presence of CO_2 in the diluent. Their physical meaning will be better explained in the following section.

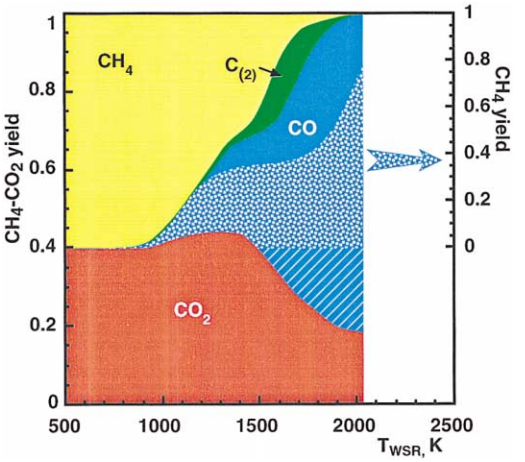

FIG. 5. Left-hand axis: red area, carbon yield to CO_2; plain, dotted, and dashed blue areas, carbon yield to CO; green area, carbon yield to $C_{(2)}$; yellow area, unconverted methane; computed by using $N_2/CO_2/H_2O$ mixture (0.65/0.067/0.133) as diluent. Right-hand axis: dotted blue area, carbon yield to CO; computed by using pure nitrogen as diluent.

Discussion

The outlet temperature of the diluted WSR of methane/air in stoichiometric conditions (C/O = 0.25) is in frozen or equilibrium conditions for a large range of inlet temperatures. In fact, Fig. 2 shows these bistable conditions for two residence times, representative of reactor conditions (τ = 0.1 s and 1 s) of practical interest. Only in a narrow range of temperatures does the passage from the two states develop at different reactor temperatures. This occurs where solution multiplicity is present; therefore, this zone does not seem to have any physical meaning. In other words, the system presents some hysteresis characteristics, but the conversion has to be considered either negligible or total. This reflects the very rapid reaction rates in the oxidation process, which are activated at reasonable delay or residence time. This condition is of no practical interest because it does not allow any intermediate state, in which interplay between different levels of oxidation can be envisaged. Decrease of the residence time down to 0.1 s (dotted line) does not significantly vary the single-value domain, apart from a slight increase of temperature in the transition region; therefore, WSR remains unfeasible for the traditional practical combustor.

Taking into account this difficulty in creating adiabatic WSRs in stoichiometic conditions, it is important to emphasize the broad variety of outlet conditions, which can be attained in the rich case (C/O = 1) of Fig. 2. The temperature exceeds the equilibrium temperature by approximately 300–400 K between the ignition condition up to T_o = 1600 K. The increase is of the same order of that related to the frozen condition, because the equilibrium and frozen temperature are quite similar in the whole investigated domain. This non-equilibrium is due to the counterbalancing effects of the exo- and endothermic transformations into oxidative and pyrolitic products. The pure pyrolitic (C/O = ∞) condition is also reported (red line) in order to stress this point. The reactor temperature is lower than the frozen temperature for T_o higher than 1500 K, since there is no exothermic oxidation, which counterbalances the endothermic pure pyrolysis.

Analysis of the conversion/yield/selectivity, reported in Figs. 3 and 4 as function of the T_{wsr}, shows the key features for understanding the non-equilibrium regime. This regime has been delimited in Fig. 4 with two dashed lines at 800 K and 1300 K. The region between these temperatures is labeled oxidation regime, because no significant pyrolitic species (e.g., C_2H_2) are produced, but only a relatively small amount of saturated (C_2H_6, C_2H_5) and unsaturated (C_2H_4, C_2H_3) compounds as well as H_2 are present. This means that the great part of the converted oxygen is evenly divided between CO and H_2O, and the residual hydrogen from the first methane molecule is mainly present in its molecular form. The unitary carbon/oxygen ratio entails the presence of two methane molecules for each oxygen molecule. Therefore, the second methane molecule undergoes a heating process, which does not yield pyrolitic reaction. Carbon conversion in this regime is only partial. A global kinetic model of the regime can be very schematically given by the following reaction at T = 1300 K

$$2CH_4 + O_2 \rightarrow CO + H_2O + H_2 + CH_4 \quad (1)$$

Attack of the methane molecule is made through radical species at this relatively low temperature, and thermal dehydrogenation is not effective. Therefore, no methyl excess can be present with respect to that formed by radicals produced by oxidation. Also, the recombination reaction rates are slower than the oxidation ones.

For T_{wsr} above 1300 K, the thermal dehydrogenation as well as CH_3 production and its recombination into C_2H_6, C_2H_5, and C_2H_4 are favored. This is possible because no competitive oxidative route is active. Therefore, one methane molecule is transformed into $C_{(2)}$ species, of which C_2H_2 is the most representative, as is shown in the selectivity profile of Fig. 4. Therefore, the second methane molecule, present as a product in equation 1, has to be substituted in the same equation with 1/2 and 3/2 molecules of acetylene and hydrogen, according to the following stoichiometry, which is quite representative of temperature around 1700 K

$$2CH_4 + O_2 \rightarrow CO + H_2O + (1 + 3/2)H_2 + 1/2C_2H_2 \quad (2)$$

The detailed analysis in terms of reaction flows, not shown here for lack of room, demonstrates that also the first CH_4 molecule undergoes dehydrogenation recombination, but in this case the acetylene is oxidized. The final result is the same as that commented on before. Therefore, the scheme outlined with equation 1 is able to take into account the main features of this regime.

The last interesting range is for T_{wsr} higher than 1700 K, and it is named pyrolitic in its precise etymological sense. Dehydrogenation seems to act directly on the $C_{(1)}$ species. This is supported by the CH_2 and CH selectivity analysis not reported here. In fact, they are present in this temperature range and originate by CH_3 dehydrogenation. In this case, the most representative overall reaction is

$$2CH_4 + O_2 \rightarrow CO + 2H_2 \quad (3)$$

From the quantitative point of view, it is approximately satisfied at $T_{wsr} > 2000$ K.

A comparison of the three regimes has to be made in terms of the technological interest in decreasing the formation of high molecular mass carbonaceous products. Acetylene can be a signature of this category, because whatever mechanism is considered for the formation of organic particles or even of the first aromatic ring, the minimum carbon aggregation is between two-carbon-atom species [15]. Acetylene formation is favored in the recombination regime at intermediate T_{wsr}, whereas it is nearly negligible below 1300 K and above 2000 K.

Finally, the effect of the oxidative stream composition can be assessed by means of Fig. 5, when the flow is diluted with an amount of CO_2 and H_2O comparable to that of the combustion products of methane.

The water shift equilibrium causes an increase of CO concentration, from the converted CO_2, shown in Fig. 5 (dashed blue region), since the molar ratio $CO/CO_2 = 1$ in the equilibrium condition. Therefore, the other part of Y_{CO} can be attributed to formation of CO from the methane. Since the dotted blue region is Y_{CO} for the N_2 diluted condition (i.e., the same as Fig. 3 but referred to the coordinate on the right side), the plain blue domain can be attributed to the methane converted to CO instead of to C_2H_2. It is clear from the comparison between Fig. 3 and Fig. 5 that the reduction of acetylene formation can be correlated with the presence of CO_2 or CO_2/H_2O dilution.

The combined partial oxidation due to oxidative species originating both from the oxygen feed at the inlet and from CO_2/O_2 reduction is the main cause of homogeneity and low luminosity in the visible wavelength range for flameless combustion. In the example reported above as well as in the few experimental cases reported in the literature [2,3,5], two simultaneous conditions are fulfilled. The first one is fuel injection in the zone, where combustion products are recirculated with a relatively low oxygen concentration. Methane is mixed with an oxygen-diluted stream, which has been modeled in the present paper with oxygen molar fraction of 0.05. Two kinds of inert (pure N_2 (0.85) as well as $N_2/CO_2/H_2O$ (0.65/0.067/0.133)) mixtures have been used in order to deduce the additional influence of flue gas composition.

The second condition is preheating of the inlet oxidant stream [2,3,5], which also induces an increase of the adiabatic flame temperature. This results in such an increase of the recirculated flue gas temperature that, even in presence of heat loss, the pure pyrolitic regime is attained. It is worthwhile to stress that acetylene is depressed in this regime and that it is further decreased when real flue gas composition is taken into account.

The hypothesis of well stirring has previously been considered to be plausible from the kinetic point of view because of the long and different characteristic times involved in the different chemical routes. This hypothesis is not restrictive because it has been used only to perform a zero dimensional analysis, which could cover a broad range of temperatures and compositions. Different process evolutions can be envisaged inside this partial oxidation stage, but they have to be limited to the very diluted rich conditions considered here. Non-uniform distribution of the air/fuel ratio can be accepted because the diffusive structures originating from this stratification cannot reach the high temperatures imposed by the preheating. This is due to the milding effect of the partial heat release (rich condition) and the high thermal capacity of the mixture (diluted conditions).

Homogeneity of heat release is not only ensured by the intensity of stirring, which can be reached in this recirculation zone, but also by the fact that this, in turn, is part of the whole process. This can be considered a staged oxidation which releases part of the combustion enthalpy in different regions of the combustor. The difference with the inert reverse flow, used for the stabilization of traditional combustors, is also made greater by the fact that these flows are sometimes lapping cold confinement walls.

The colorless characteristics are mainly due to the two-staged evolution. The first one yields combustible species such as CO and H_2, which in turn are known to support flames with low visible luminosity. In the first stage, the possible production of some chemiluminescent CH_2 and CH radicals are also quite small, because they are formed by the reduced dehydrogenation of the single-atom saturated species, which has been shown to be quite low.

Sometimes greenish flames have been detected [2,16] in the high-temperature air combustion of

propane, which was mainly attributed to C_2 radicals. These radicals can be formed through recombination, as is shown in this paper, but also through fragmentation of heavier paraffins, like the propane itself.

Conclusion and Final Remarks

Flameless combustion has been shown to be consistent with two-stage oxidation, in which the first part is in rich diluted conditions. There are four parts to the evidence. The first two refer to similarity in the inlet process condition, namely, the high temperature of the reactant mixture and the injection of the fuel in the flue gas with low oxygen content. The other two refer to the unusual properties of the process, that is, the low visible emission of the process and the uniformity due to both the staged process and the well stirring in the oxidative–pyrolitic condition.

This evidence is based on the grounds of a comprehensive kinetic study of different possible routes. Each of these parts of the mechanism is well known in the literature because they refer to well-identified technological fields and basic disciplines. This is one of the reasons why the methane mechanism could benefit from an enormous amount of kinetic data and could be validated in several ranges of applications. At the same time, this makes the analysis of the single process not particularly interesting, whereas the screening in such a wide range of temperature/composition is of great importance, particularly with respect to innovative combustion processes, in which different variables are simultaneously changed.

Even though the original mechanism was mainly developed for methane oxidation, the crucial recombination step is included, and the primary kinetics for pyrolysis can therefore be evaluated. Furthermore, the whole scheme is well referenced [9], and it can be considered as standard so that process assessments are obtained by objective, verifiable procedures.

Apart from the rational analysis of flameless combustion, some other processes can be optimized in terms of the selectivity adjustments according to the regimes identified in this paper. In particular, the oxidation one is of interest in reburning technology, because it is quite similar to WSR conditions in terms of temperature and composition. The same is also true for combustion with a high level of external recirculation, which is thought capable of creating conditions of mild combustion suitable for NO_x reduction and abatement.

Acknowledgments

The authors wish to acknowledge the ENEL-Area Ricerca for the financial support and Ing. Raffaele Donnarumma and Ing. Gabriella Anniciello for their help in the elaboration of some results.

REFERENCES

1. Katsuki, M., and Hasegawa, T., *Proc. Combust. Inst.* 27:3135–3146 (1998).
2. Ishiguro, T., Tsuge, S., Furuhata, T., Kitigawa, K., Arai, N., Hasegawa, T., Tanaka, R., and Gupta, A. K., *Proc. Combust. Inst.* 27:3205–3213 (1998).
3. Plessing, T., Peters, N., and Wünning, J. G., *Proc. Combust. Inst.* 27:3197–3204 (1998).
4. Yasuda, T., *Proceedings of Second Int. High Temperature Air Combustion Symp.,* Taiwan, p. B3, 1999.
5. Weber, R., *Proceedings of Second Int. High Temperature Air Combustion Symp.,* Taiwan, p. C2, 1999.
6. Wünning, J. A., and Wünning, J. G., *Prog. Energy Combust. Sci.* 23:81–94 (1997).
7. de Joannon, M., Langella, G., Beretta, F., Cavaliere, A., and Noviello, C., *Proceedings of Technology and Combustion for Clean Environment,* Lisbon, Portugal, 1999, pp. 435–442.
8. Smith, G., Golden, D., Frenklach, M., Moriarty, N. W., Eiteneer, B., Goldenberg, M., Bowman, T. C., Hanson, R., Song, S., Gardiner, C., Lissianski, V., and Qin, Z., http://www.me.berkeley.edu/gri_mech/, University of California, Berkeley, CA, Oct. 16, 2000.
9. Warnatz, J., Maas, U., and Dibble, R. W., *Combustion: Physical and Chemical Fundamentals, Modelling and Simulation, Experiments, Pollutant Formation, 2nd ed.,* Berlin, Springer, 1999.
10. Gaffuri, P., Faravelli, T., Ranzi, E., Cernansky, N. P., Miller, D., D'Anna, A., and Ciajolo, A., *AIChE J.* 43(5):1278–1286 (1997).
11. Warnatz, J., http://www.ca.sandia.gov/tdf/3rdWorkshop/ch4mech.html. Sandia National Laboratories, Livermore, CA, Oct. 16, 2000.
12. Glarborg, P., Kee, R. J., Grcar, J. F., and Miller, J. A., Sandia report SAND 86-8209.
13. Kee, R. J., Rupley, F. M., and Miller, J. A., Sandia report SAND 89-8009B.
14. Tan, Y., Dagaut, P., Cathonnet, M., and Boettner, J. C., *Combust. Sci. Technol.* 102:21–55 (1994).
15. Miller, J. A., and Melius, C. F., *Combust. Flame* 91:21–39 (1992).
16. Bolz, S., and Gupta, A. K., *ASME Fact* 22:193–206 (1998).

COMMENTS

Bassam Dally, University of Adelaide, Australia. You showed the effects of CO_2 addition to the mixture. How will the addition of H_2O to the mixture affect the oxidation of soot precursors in the mixture?

You suggested to use the technology as a postprocess to burn soot. How would this technology be applied for NO_x reburn?

Author's Reply. In this work, we have shown that the addition of CO_2 and H_2O to the diluent in fuel-rich oxidation leads to the reduction of C_2H_2, which is not considered here as a soot precursor. Both CO_2 and H_2O behave in a similar way as diluents, increasing the concentration of radicals acting as a C_2H_2 oxidizer. In fact, CO_2 directly decomposes to CO and O [1], whereas H_2O presence shifts the reaction network, in which H_2O is involved, toward the formation of such radicals.

An interpretation of this phenomenology could suggest the conclusive statement that any species added as diluent able to form radicals involved in acetylene oxidation leads to the C_2H_2 reduction.

REFERENCE

1. Cavaliere, A., and de Joannon, M., Proceedings of 3rd Int. Symposium on High Temperature Air Combustion and Gasification, Yokohama, Japan, March 7–9, 2000.

•

Roman Weber, International Fire Research Foundation, The Netherlands. What is the significance of the presence of C_2 radicals in such large quantities?

Author's Reply. In the Warnatz model, the dehydrogenation reaction of C_2H_2 leading to C_2 is not considered. Therefore, we limited our attention to C_2H_2. However, it could be possible that such quantities of C_2H_2 cause the massive formation of C_2 radicals, responsible for the characteristic green emission of the high-temperature-diluted combustion. It is noteworthy to underline that an experimental study reported in the literature [1] has shown the C_2 chemiluminescence reduction in high-temperature-diluted combustion when CO_2 is added to the diluent. This is in agreement with the C_2H_2 reduction obtained in the present work CO_2 dilution effects.

REFERENCE

1. Shimo, N., Proceedings of 2nd Int. Seminar on High Temperature Combustion in Industrial Furnaces, Stockholm, Sweden, January 17–18, 2000.